Su *et al. J Wireless Com Network* (2025) 2025:10
https://doi.org/10.1186/s13638-025-02428-1

EURASIP Journal on Wireless Communications and Networking

RESEARCH Open Access

Secure ISAC MIMO systems: exploiting interference with Bayesian Cramér–Rao bound optimization

Nanchi Su[1,2,3*], Fan Liu[2], Christos Masouros[3], George C. Alexandropoulos[4], Yifeng Xiong[5] and Qinyu Zhang[1,6]

*Correspondence:
sunanchi@hit.edu.cn

[1] Guangdong Provincial Key Laboratory of Aerospace Communication and Networking Technology, Harbin Institute of Technology (Shenzhen), Shenzhen 518055, China
[2] School of System Design and Intelligent Manufacturing, Southern University of Science and Technology, Shenzhen 518055, China
[3] Department of Electronic and Electrical Engineering, University College London, London WC1E 7JE, UK
[4] Department of Informatics and Telecommunications, National and Kapodistrian University of Athens, 15784 Athens, Greece
[5] School of Information and Electronic Engineering, Beijing University of Posts and Telecommunications, Beijing 100876, China
[6] Peng Cheng Laboratory, Shenzhen 518055, China

Abstract

In this paper, we present a signaling design for secure integrated sensing and communication (ISAC) systems comprising a dual-functional multi-input multi-output base station that simultaneously communicates with multiple users while detecting targets present in their vicinity, which are regarded as potential eavesdroppers. In particular, assuming that the distribution of each parameter to be estimated is known *a priori*, we focus on optimizing the targets' sensing performance. To this end, we derive and minimize the Bayesian Cramér–Rao bound, while ensuring certain communication quality of service by exploiting constructive interference. The latter scheme enforces that the received signals at the eavesdropping targets fall into the destructive region of the signal constellation, to deteriorate their decoding probability, thus enhancing the ISAC's system physical layer security capability. To tackle the nonconvexity of the formulated problem, a tailored successive convex approximation method is proposed for its efficient solution. Our extensive numerical results verify the effectiveness of the proposed secure ISAC design showing that the proposed algorithm outperforms block-level precoding techniques.

Keywords: Integrated sensing and communication, Physical layer security, Successive convex approximation, Bayesian Cramér–Rao bound, Constructive interference

1 Introduction

Future radar and communication (R&C) systems will operate at higher frequencies with larger bandwidth, while possibly exploiting massive antenna arrays and multi-functional reconfigurable intelligent surfaces (RIS), resulting in striking similarities between R&C systems, including the hardware architecture, channel characteristics, and signal processing methods [1, 2]. This provides unique opportunities to develop co-design techniques aiming at improving the mutual performance gain of both systems. Meanwhile, with the emergence of smart cities, Internet of Things (IoT) networks, and other advanced applications, the integration of sensing and communication (S&C) systems is being seen as a transformative technology, enabling autonomous vehicle networks, activity recognition, and unmanned aerial vehicle (UAV) [3].

Springer Open

© The Author(s) 2025. **Open Access** This article is licensed under a Creative Commons Attribution 4.0 International License, which permits use, sharing, adaptation, distribution and reproduction in any medium or format, as long as you give appropriate credit to the original author(s) and the source, provide a link to the Creative Commons licence, and indicate if changes were made. The images or other third party material in this article are included in the article's Creative Commons licence, unless indicated otherwise in a credit line to the material. If material is not included in the article's Creative Commons licence and your intended use is not permitted by statutory regulation or exceeds the permitted use, you will need to obtain permission directly from the copyright holder. To view a copy of this licence, visit http://creativecommons.org/licenses/by/4.0/.

In light of the above, the need for seamless cooperation between S&C promotes the technical development of integrated sensing and communication (ISAC) systems.

The utilization of a communal spectrum frequency band, coupled with the intrinsic broadcasting characteristics of wireless transmission, introduces substantial security vulnerabilities in ISAC systems [4–6]. In conventional wireless communication systems, security designs are predominantly concerned at the physical layer and the network layer. Compared with network layer security (NLS), physical layer security (PLS) does not require complex cryptographic techniques or key distribution, reducing overhead and complexity. Moreover, PLS may provide a base level of security guarantee even when other layers are compromised, because it leverages the physical characteristics of wireless channels, which are independent of security at other layers of the communication stack.

The PLS in ISAC systems has been widely studied in recent years. Initially, the artificial noise (AN) is deployed to interfere with eavesdroppers by maximizing the secrecy rate; thus, the target/eavesdropper is unable to decode the received signal. To this end, the confidential information is prevented from being intercepted by the target/eavesdropper [5, 7–9]. Besides, the authors in [10] expand the AN-aided technique to full-duplex ISAC security, where the AN is utilized to enhance both downlink (DL) and uplink (UL) secrecy rates in the presence of multiple eavesdroppers. The work presents a power-efficient optimization model that maximizes UL/DL secrecy while targeting radar beams at eavesdroppers to extract their physical parameters, revealing key trade-offs between sensing performance and communication security. Moreover, the directional modulation (DM) technique, which is based on the principle of constructive interference (CI), has been deployed to design the transmit signal at a symbol level [11–13]. In DM, as a step further from AN design, the signals received at multiple eavesdropping targets (Eves) are enforced to fall into the destructive constellation region for further PLS improvements, which leverages destructive interference (DI) as a PLS measure. In particular, the CI-DI technique enables direct alteration of the amplitude and phase of signals at both intended users and potential Eves. Consequently, this paradigm promotes an enhanced symbol error rate (SER) for communication users (CUs), while deteriorating the decoding probability at potential eavesdroppers.

In this work, we consider the estimation task of random parameters of multiple targets, where the prior distribution of parameters is assumed to be known *a priori*. This is common in a number of practical scenarios, such as vehicle tracking and environmental monitoring. Toward that aim, we then evaluate the sensing performance utilizing the lower bound of the unbiased estimation, i.e., Bayesian Cramér–Rao bound (BCRB). Specifically, we formulate a novel signaling design problem that aims to minimize the BCRB, while guaranteeing a predefined quality of service (QoS) at the multiple CUs, by deploying the CI technique and improving the PLS by constraining the received signals at targets/Eves in the destructive constellation region. Moreover, we explore the impact of the *a priori* distribution of the parameters on the radar

beampattern as well as the performance trade-off between the sensing and communication operations. For further clarity, the insights of this work are summarized as follows:

- This work not only derives the BCRB for the estimation of random target parameters within an ISAC system, but also proposes an optimization strategy specifically tailored to minimize this bound while meeting stringent QoS requirements for multiple users. This focus on minimizing BCRB for ISAC applications is, to our knowledge, a novel contribution that directly addresses the sensing performance, particularly under security constraints.
- Although the concept of using CI-DI for security is not new, our approach adapts this for ISAC by introducing a three-zone division within the destructive region, providing a structured solution to manage the nonconvexity of the constraints. This adaptation is particularly tailored to the needs of ISAC systems, where communication and sensing objectives are tightly integrated.
- Unlike previous studies [14] that focus on single-target detection, our work extends the application to a multi-target scenario. By considering multiple targets as potential eavesdroppers, we develop an optimization strategy that ensures robust communication security while enhancing the overall sensing capabilities of ISAC systems.

Notations: Unless otherwise specified, matrices are denoted by bold uppercase letters (i.e., $\mathbf{X}$), vectors are represented by bold lowercase letters (i.e., $\mathbf{x}$), and scalars are denoted by normal font (i.e., α). Subscripts indicate the location of the entry in the matrices or vectors (i.e., $s_{i,j}$ and l_n are the (i, j)-th and the n-th element in $\mathbf{S}$ and $\mathbf{l}$, respectively). $\otimes$ denotes the Kronecker product. tr $(\cdot)$ and vec $(\cdot)$ denote the trace and the vectorization operations. $(\cdot)^T$, $(\cdot)^H$, and $(\cdot)^*$ stand for transpose, Hermitian transpose, and the complex conjugate of the matrices, respectively. $\|\cdot\|$, $\|\cdot\|_\infty$ and $\|\cdot\|_F$ denote the l_2 norm, infinite norm, and the Frobenius norm, respectively. $\mathbb{E}\{\cdot\}$ denotes the statistical expectation.

2 Methods and results

2.1 Signal model

As shown in Fig. 1, we consider a downlink multi-user multi-input single-output (MU-MISO) wireless system, where the dual-functional multi-input multi-output (MIMO) base station (BS) is capable of detecting multi-targets simultaneously with

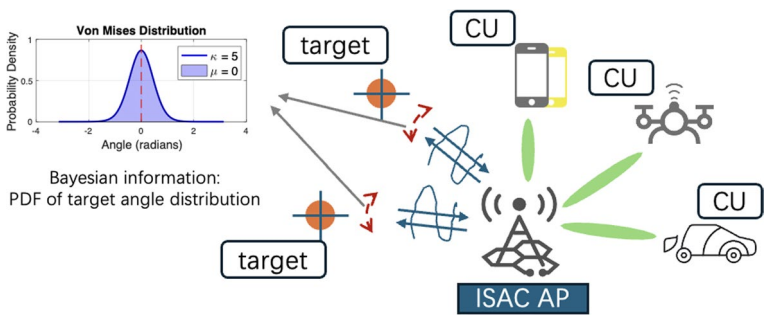

Fig. 1 The considered system model comprising multiple communication users (CUs) and multiple targets in the vicinity of an ISAC access point (AP)

data transmission. The targets are treated as potential Eves of the communication information. The BS is equipped with N_t transmit antennas and N_r receive antennas, enabling communication with K_{cu} single-antenna users and detection of K_{tar} targets of interest[1]. Below we elaborate on the signal models of both radar and communication systems, respectively.

Let $\mathbf{X} \in \mathbb{C}^{N_t \times L}$ denote the dual-functional signal matrix, where $\mathbf{X} = [\mathbf{x}[1], \mathbf{x}[2], \ldots, \mathbf{x}[L]]$, each element of which denotes the transmit signal vector at the l-th time slot with $l = 1, 2, \ldots, L$. Then, the received signal at each k-th single-antenna CU, with $k = 1, 2, \ldots, K_{cu}$, at the l-th time slot is given as

$$y_{\mathrm{CU,k}}[l] = \mathbf{h}_{\mathrm{CU,k}}^H \mathbf{x}[l] + z_{\mathrm{CU,k}}[l], \tag{1}$$

where $\mathbf{h}_{\mathrm{CU,k}}^H \in \mathbb{C}^{N_t \times 1}$ denotes the MISO channel vector between the BS and the k-th CU, and the complex-valued $z_{\mathrm{CU,k}}[l]$ denotes the zero-mean additive white Gaussian noise (AWGN) with the variance of each entry being $\sigma_{\mathrm{CU,k}}^2$. According to the paradigm of the CI technique [14, 17], the SNR per frame of the k-th CU is given as

$$\mathrm{SNR}_{\mathrm{CU,k}} = \frac{\mathbb{E}\left[\left|\mathbf{h}_{\mathrm{CU,k}}^H \mathbf{x}[l]\right|^2\right]}{\sigma_{\mathrm{CU,k}}^2}. \tag{2}$$

On the other hand, the sensing signal model can be mathematically expressed as follows:

$$\mathbf{Y}_S = \mathbf{H}_S(\boldsymbol{\eta})\mathbf{X} + \mathbf{Z}_S, \tag{3}$$

where $\mathbf{Y}_S \in \mathbb{C}^{N_r \times L}$, $\mathbf{Z}_S$ represents the AWGN with zeros-mean complex-value elements each with the variance of σ_S^2, and $\mathbf{H}_S \in \mathbb{C}^{N_r \times N_t}$ denotes the target response matrix, which is a function of the physical parameters $\boldsymbol{\eta} \in \mathbb{R}^M$ to be estimated, including range, angle, and Doppler, with M denoting the number of parameters to be estimated. In this paper, we consider a particular case of channel matrix $\mathbf{H}_S$, which is expressed as

$$\mathbf{H}_S = \sum_{n=1}^{K_{tar}} \alpha_n \mathbf{b}(\theta_n)\mathbf{a}^H(\theta_n), \tag{4}$$

where α_n denotes the channel coefficient of each target, consisting of both the radar cross section (RCS) and path loss, which obeys the complex Gaussian distribution, and $\mathbf{a}(\theta)$, $\mathbf{b}(\theta)$ represent the transmit and receive steering vector, respectively. The received signal at the n-th target/Eve is accordingly written as

$$\mathbf{y}_{\mathrm{E,n}} = \beta_n \mathbf{a}^H(\theta_n)\mathbf{X} + \mathbf{e}_n, \tag{5}$$

[1] From the sensing side, we assume that one sub-array (consisting of N_t antennas) is deployed to transmit signals and another sub-array (comprising N_r antennas) is deployed to receive signals. These sub-arrays are co-located at the BS and operated simultaneously to transmit the dual-function signal and receive its echoes for monostatic sensing. In principle, the transmitted signal will interfere with the reflected echoes (arriving with a round-trip propagation delay) at the receive sub-array, creating a self-interference signal at the BS. This is a typical problem in full-duplex (FD) BSs used for simultaneous communications and sensing [15]. Fortunately, there exist various approaches for efficiently suppressing self-interference below the noise floor in multi-antenna FD systems, ranging from isolation between the transmit and receive arrays to joint digital and analog beamforming and interference cancellation techniques. Capitalizing on this, in the paper, we neglect the impact of the self-interference assuming that it can be efficiently handled via the state-of-the-art approaches [15, 16].

where $\beta_n, \forall\, n$ denotes the path loss of the n-th target/Eve, and $\mathbf{e}_n$ denotes the zero-mean AWGN vector, with the variance of each entry being $\sigma^2_{\mathrm{E,n}}$.

Given the channel model (4), we define the vector with the unknown targets' parameters $\boldsymbol{\eta} = [\mathrm{Re}\{\boldsymbol{\alpha}\}, \mathrm{Im}\{\boldsymbol{\alpha}\}, \boldsymbol{\theta}] \in \mathbb{C}^{N\times 3}$, with $\boldsymbol{\alpha} = [\alpha_1, \ldots, \alpha_N]^T, \boldsymbol{\theta} = [\theta_1, \ldots, \theta_N]^T$. The steering vector and its derivative are specified as (assuming an even number of antennas):

$$\begin{aligned}\mathbf{a}(\theta) &= \left[e^{-j\pi \frac{N_t-1}{2}\sin(\theta)}, e^{-j\pi \frac{N_t-3}{2}\sin(\theta)}, \ldots, e^{j\pi \frac{N_t-1}{2}\sin(\theta)}\right]^T,\\ \mathbf{Pa}(\theta) &= \left[-j\pi \frac{N_t-1}{2}\cos(\theta)a_1, \ldots, j\pi \frac{N_t-1}{2}\cos(\theta)a_{N_t}\right]^T,\end{aligned} \tag{6}$$

where a_n, with $n = 1, \ldots, N_t$ denotes the n-th element of the steering vector $\mathbf{a}(\theta)$. Here, we choose the center of the ULA as a phase reference, such that

$$\mathbf{a}^H\mathbf{Pa} = 0, \mathbf{b}^H\mathbf{Pb} = 0. \tag{7}$$

Accordingly, the covariance matrix of the dual-functional transmitted signal is given as

$$\mathbf{R}_x = \frac{1}{L}\mathbf{X}\mathbf{X}^H = \frac{1}{L}\sum_{l=1}^{L}\mathbf{x}[l]\mathbf{x}^H[l]. \tag{8}$$

For the sensing performance metric, we employ the estimation mean-squared error (MSE) of $\boldsymbol{\eta}$, which is bounded by the CRB. By denoting the estimation of $\boldsymbol{\eta}$ as $\hat{\boldsymbol{\eta}}$, we have that:

$$\mathrm{MSE}_{\boldsymbol{\eta}}\left(\hat{\boldsymbol{\eta}}\right) \geq \mathrm{tr}\left(\mathbf{J}^{-1}\right), \tag{9}$$

where $\mathbf{J}$ is the Bayesian Fisher Information Matrix (BFIM) of $\boldsymbol{\eta}$ which is defined as follows:

$$\begin{aligned}\mathbf{J} =& \mathbb{E}_{\boldsymbol{\eta}}\left\{\frac{\partial \ln p_{\mathbf{Y}_S|\boldsymbol{\eta}}(\mathbf{Y}_S|\boldsymbol{\eta})}{\partial \boldsymbol{\eta}}\frac{\partial \ln p_{\mathbf{Y}_S|\boldsymbol{\eta}}(\mathbf{Y}_S|\boldsymbol{\eta})}{\partial \boldsymbol{\eta}^T}\right\}\\ &+\mathbb{E}_{\boldsymbol{\eta}}\left\{\frac{\partial \ln p_{\boldsymbol{\eta}}(\boldsymbol{\eta})}{\partial \boldsymbol{\eta}}\frac{\partial \ln p_{\boldsymbol{\eta}}(\boldsymbol{\eta})}{\partial \boldsymbol{\eta}^T}\right\},\end{aligned} \tag{10}$$

where $p_{\boldsymbol{\eta}}(\boldsymbol{\eta})$ denotes the prior distribution of the parameters' vector $\boldsymbol{\eta}$, and $p_{\mathbf{Y}_S|\boldsymbol{\eta}}(\mathbf{Y}_S|\boldsymbol{\eta})$ is the probability of observing the data $\mathbf{Y}_S$ given the parameter $\boldsymbol{\eta}$. To derive the BFIM, we firstly let $\mathbf{y}_S = \mathrm{vec}\left(\mathbf{Y}_S^T\right)$, and thus, the sensing signal model can be rewritten as

$$\mathbf{y}_S = \left(\mathbf{I}_{N_r} \otimes \mathbf{X}^T\right)\mathrm{vec}\left(\mathbf{H}_S^T\right) + \mathrm{vec}\left(\mathbf{Z}_S^T\right). \tag{11}$$

Then, let $\mathbf{h}_S = \left[\mathrm{vec}\left(\mathbf{H}_S^T\right)^T, \mathrm{vec}\left(\mathbf{H}_S^T\right)^H\right]$ and $\mathbf{F} = \frac{\partial \mathbf{h}_S^*}{\partial \boldsymbol{\eta}} \in \mathbb{C}^{K\times 2N_tN_r}$. We further partition $\mathbf{F}$ as

$$\mathbf{F} = \left[\,\mathbf{F}_1, \ldots, \mathbf{F}_{2N_r}\,\right], \tag{12}$$

where $\mathbf{F}_i \in \mathbb{C}^{K\times N_t}$, with $i = 1, \ldots, 2N_r$. Accordingly, the BFIM can be rewritten as [18]

$$\begin{aligned}\mathbf{J} &= \frac{L}{\sigma_s^2}\left\{\mathbb{E}_\eta\left\{\mathbf{F}\begin{bmatrix}\mathbf{I}_{N_r}\otimes\mathbf{R}_x^T & \mathbf{0}\\ \mathbf{0} & \mathbf{I}_{N_r}\otimes\mathbf{R}_x\end{bmatrix}\mathbf{F}^H\right\}+\mathbf{J}_P\right\}\\ &= \frac{L}{\sigma_s^2}\left\{\mathbb{E}_\eta\left\{\sum_{i=1}^{N_r}\left(\mathbf{F}_i\mathbf{R}_x^T\mathbf{F}_i^H+\mathbf{F}_{N_r+i}\mathbf{R}_x\mathbf{F}_{N_r+i}^H\right)\right\}+\mathbf{J}_P\right\}\end{aligned} \tag{13}$$

where $\mathbf{J}_P$ depends on the *a priori* distribution $p_\eta(\eta)$.

To deal with the expectation operation in (14), we define the following matrices:

$$\boldsymbol{A}_1(\boldsymbol{\Xi}) = \sum_{i=1}^{N_r}\mathbf{F}_i\boldsymbol{\Xi}\mathbf{F}_i^H, \tag{14a}$$

$$\boldsymbol{A}_2(\boldsymbol{\Xi}) = \sum_{i=1}^{N_r}\mathbf{F}_{N_r+i}\boldsymbol{\Xi}\mathbf{F}_{N_r+i}^H. \tag{14b}$$

To derive the expectation of the later matrices, we start with (14a) and define the auxiliary matrices:

$$\boldsymbol{B}_1 = \sum_{i=1}^{N_r}\mathrm{vec}(\mathbf{F}_i)\mathrm{vec}(\mathbf{F}_i)^H, \tag{15a}$$

$$\mathbf{N}_{\mathbf{B}_1} = \mathbb{E}\{\mathbf{B}_1\} = \sum_{i=1}^{N_r}\mathbb{E}\{\mathrm{vec}(\mathbf{F}_i)\mathrm{vec}(\mathbf{F}_i)^H\}, \tag{15b}$$

where the latter's eigenvalue decomposition is defined as:

$$\mathbf{N}_{\mathbf{B}_1} = \mathbf{U}_1\Lambda_1\mathbf{U}_1^H = \sum_{i=1}^{r_1}\left(\sqrt{\lambda_i}\mathbf{u}_i\right)\left(\sqrt{\lambda_i}\mathbf{u}_i\right)^H, \tag{16}$$

where $\mathbf{u}_i$ denotes the corresponding eigenvector of λ_i, with $i = 1\ldots,r_1$. We assume that $\lambda_1 \geq \lambda_2,\ldots,\lambda_{MN_t}$ and let r_1 denote the number of nonzero elements in Λ_1. It can be easily shown that

$$\mathbb{E}\{\boldsymbol{A}_1(\boldsymbol{\Xi})\} = \sum_{i=1}^{r_1}\mathbf{Q}\quad\mathbf{F}_i\boldsymbol{\Xi}\quad\mathbf{Q}\quad\mathbf{F}_i^H, \tag{17}$$

where $\tilde{\mathbf{F}}_i = \sqrt{\lambda_i}\mathrm{mat}(\mathbf{u}_i)$.

Likewise, we have $\mathbb{E}\{\mathbf{A}_2(\boldsymbol{\Xi})\} = \sum_{i=1}^{r_2}\tilde{\mathbf{G}}_i\boldsymbol{\Xi}\tilde{\mathbf{G}}_i^H$, where $\tilde{\mathbf{G}}_i = \sqrt{\bar{\lambda}_i}\mathrm{mat}(\bar{\mathbf{u}}_i)$, as derived from (14b). To this end, the BFIM is consequently reformulated as follows:

$$\mathbf{J} = \frac{L}{\sigma_s^2}\left(\sum_{i=1}^{r_1}\tilde{\mathbf{F}}_i\mathbf{R}_x^T\tilde{\mathbf{F}}_i^H+\sum_{j=1}^{r_2}\tilde{\mathbf{G}}_j\mathbf{R}_x\tilde{\mathbf{G}}_j^H\right)+\mathbf{J}_P. \tag{18}$$

Therefore, the BCRB with respect to $\boldsymbol{\eta}$ is accordingly given as

$$\text{BCRB} \triangleq \text{tr}\left(\mathbf{J}^{-1}\right). \tag{19}$$

2.2 Problem formulation

Given the simplified expression of the BFIM, we are now ready to formulate the optimization problem to minimize the BCRB, while conveying the received signals at CUs into the constructive region and constraining the transmit power by designing the signal matrix $\mathbf{X}$. Moreover, the received signals at targets/Eves are limited in the destructive region for the communication data security concern. Inspired by the CI-DI technique proposed in [14, 17], the BCRB minimization problem is formulation as follows

$$\min_{\mathbf{X}} \quad \text{tr}\left(\mathbf{J}^{-1}\right) \tag{20a}$$

$$\text{s.t.} \quad \frac{1}{L}\|\mathbf{X}\|_F^2 \leq P_T, \tag{20b}$$

$$\left|\text{Im}\left(\mathbf{Q} \quad \mathbf{h}_{\text{CU},k}^H \mathbf{X}\right)\right| \leq \left(\text{Re}\left(\mathbf{Q} \quad \mathbf{h}_{\text{CU},k}^H \mathbf{X}\right) - \sqrt{\sigma_{\text{CU},k}^2 \Gamma_{\text{CU},k}}\right) \tan\phi, \forall\, k, \tag{20c}$$

$$\left|Im\left(\beta_n \mathbf{Q}\mathbf{a}^H(\theta_n)\mathbf{X}\right)\right| \geq \left(Re\left(\beta_n \mathbf{Q}\mathbf{a}^H(\theta_n)\mathbf{X}\right) - \tau_{\text{E,n}}\right) \tan\phi, \forall\, n, \tag{20d}$$

where $\tilde{\mathbf{h}}_{\text{CU,k}}^H = \mathbf{h}_{\text{CU,k}}^H s_k^*$, and $\tilde{\mathbf{a}}^H(\theta_n) = \mathbf{a}^H(\theta_n)s_1^*$ by taking the symbol s_1 as a reference. P_T denotes the transmit power budget, $\Gamma_{\text{CU,k}}, \forall\, k$ is the given SNR thresholds for CUs, and $\tau_{\text{E,n}}$ is the given scalar for limiting the targets' received symbols in the DI region. Note that $\tau_{\text{E,n}}$ is generally set much smaller than the CUs' SNR threshold $\Gamma_{\text{CU,k}}, \forall\, k$. We assume that the intended signals are M-Phase-shift keying (PSK) modulated, and thus, $\phi = \pm\pi/M$. The constraint (20c) limits the signals received by CUs within the constructive region, while (20d) limits the received signals being distributed out of the constructive region. This makes correct detection more challenging for the targets by designing the received signals' constellation, meanwhile reducing the eavesdropping SINR [14, 19, 20].[2]

Note that the nonconvexity of problem (20) lies in the objective function and the constraint (20d). Following the method presented in [14], we divide the destructive region into three zones; that is, the inequality (20d) holds when any one of the following constraints is fulfilled.

[2] The eavesdropping SINR at the n-th target/Eve regarding the k-th CU is expressed as $\text{SINR}_{n,k}^E = \frac{\mathbb{E}\left[\left|\beta_n \mathbf{a}^H(\theta_n)\mathbf{x}[l]\right|^2\right]}{\mathbb{E}\left[\left|\beta_n \mathbf{a}^H(\theta_n)\mathbf{x}[l] - s_{k,l}\right|^2\right] + \sigma_{E,n}^2}$, where $s_{k,l}$ denotes the desired constellation symbol for the k-th CU at the l-th time slot. It is easy to note that the $\text{SINR}_{n,k}^E$ is constrained once the inequality (20d) is satisfied.

case 1:

$$Re\left(\beta_n \mathbf{a}^H(\theta_n)\mathbf{X}\right) \leq \tau_{\mathrm{E,n}},$$

case 2:

$$Im\left(\beta_n \mathbf{a}^H(\theta_n)\mathbf{X}\right) \geq \left(Re\left(\beta_n \mathbf{a}^H(\theta_n)\mathbf{X}\right) - \tau_{\mathrm{E,n}}\right)\tan\phi$$

and $Re\left(\beta_n \mathbf{a}^H(\theta_n)\mathbf{X}\right) > \tau_{\mathrm{E,n}}$,

case 3:

$$-Im\left(\beta_n \mathbf{a}^H(\theta_n)\mathbf{X}\right) \geq \left(Re\left(\beta_n \mathbf{a}^H(\theta_n)\mathbf{X}\right) - \tau_{\mathrm{E,n}}\right)\tan\phi$$

and $Re\left(\beta_n \mathbf{a}^H(\theta_n)\mathbf{X}\right) > \tau_{\mathrm{E,n}}$.

Till now, (20d) is rewritten as three linear constraints; that is, problem (20) is converted to three subproblems. We solve each subproblem, and the one that results in the minimum value of the BCRB is the final solution to problem (20). However, the objective function is still nonconvex. In the following section, we present an efficient solver following the successive convex approximation (SCA) approach.

2.3 Proposed secure ISAC signaling design

Algorithm 1 SCA Algorithm for Solving (20)

Input: $\mathbf{H}, P_T, \Gamma_k, \forall\, k, K_{cu}, K_{tar}, \mathbf{J}_p, \epsilon > 0$, and the maximum iteration number n_{max}
Output: $\mathbf{X}$
Initialization: Initialize $\mathbf{X}^0 \in \mathcal{Q}$, and set $n = 1$.
1: **repeat**
2: Calculate the gradient $\nabla f\left(\mathbf{X}^{n-1}\right)$.
3: Rewrite the problem (20) as three subproblems by dividing the destructive region into three zones, and obtain the optimal solutions $\mathbf{X_1}^*, \mathbf{X_2}^*$, and $\mathbf{X_3}^*$.
4: Update the solutions by (23), where λ can be obtained by deploying the Armijo search or the exact line search.
5: $n = n + 1$.
6: **until** $g\left(\mathbf{X}^i\right) > -\epsilon$ or $n > n_{max}$.
7: Calculate the value of the objective function utilizing the obtained $\mathbf{X_1}^*, \mathbf{X_2}^*$, and $\mathbf{X_3}^*$, and choose the one that results in the minimum BCRB as the final solution to problem (20).
8: end

We note that the constraints in problem (20) are all convex, while the objective function is nonconvex. To this end, we define $\mathcal{Q}$ as the feasible region of problem (20), which is convex. To tackle the problem, let us denote the objective function as $f(\mathbf{X}) \triangleq \mathrm{tr}\left(\mathbf{J}^{-1}\right)$. Then, we approximate the objective function by its first-order Taylor expansion near a given point $f\left(\mathbf{X}'\right)$, yielding

$$f(\mathbf{X}) \approx f\left(\mathbf{X}'\right) + \mathrm{Re}\left(\mathrm{tr}\left(\nabla f^H\left(\mathbf{X}'\right)\left(\mathbf{X} - \mathbf{X}'\right)\right)\right), \tag{21}$$

where $\nabla f(\cdot)$ denotes the gradient of $f(\cdot)$. Note that the first term in (21) is a constant, hence, we can equivalently solve the following optimization problem at the n-th iteration of the SCA solver:

$$\begin{aligned} &\min_{\mathbf{X}} g(\mathbf{X}) \triangleq \mathrm{Re}\Big(\mathrm{tr}\Big(\nabla f^H\Big(\mathbf{X}^{n-1}\Big)\Big(\mathbf{X}-\mathbf{X}^{n-1}\Big)\Big)\Big) \\ &\text{s.t. (20b) to (20d),} \end{aligned} \tag{22}$$

where $\mathbf{X}^{n-1} \in \mathcal{Q}$ is the optimal signal at the $(n-1)$-th algorithmic iteration. By solving problem (22), we obtain the optimal solution, which is denoted as $\mathbf{X}^* \in \mathcal{Q}$. Here, the term $\mathbf{X}^* - \mathbf{X}^{(n-1)}$ yields a descent direction for each iteration. By letting the variable move along the descent direction with a stepsize λ, we have

$$\mathbf{X}^i = \mathbf{X}^{i-1} + \lambda\Big(\mathbf{X}^* - \mathbf{X}^{i-1}\Big), \tag{23}$$

where the stepsize λ may be obtained by adopting the Armijo search or the exact line search [21], and $\mathbf{X}^i \in \mathcal{Q}$. It is notable that the performance of the SCA technique is inevitably impacted by the initial point $\mathbf{X}^0$. In this problem, the initial point can be found by solving the following optimization problem

$$\begin{aligned} &\max_{\mathbf{X}} \mathrm{Re}(\mathrm{tr}(\mathbf{X})) \\ &\text{s.t. (20b) to (20d),} \end{aligned} \tag{24}$$

which will provide a solution close to the minimizer of the original problem (20) since it falls into the same feasibility region. For clarity, the SCA method applied to solving problem (20) is summarized in Algorithm 1.

2.4 Numerical results and discussion

In this section, numerical results are presented based on Monte Carlo simulations of the proposed optimization technique, i.e., CI-based BCRB optimization. Without loss of generality, we set $N_t = 12$, $N_r = 10$, and $L = 100$. The communication channel is assumed to be Rayleigh fading, where each entry of the channel gain vector $\mathbf{h}_{\mathrm{CU,k}}^H, \forall\, k$ is subject to the standard complex Gaussian distribution. Regarding the prior distribution of the parameters to be estimated, we assume that the propagation loss $\alpha_n, \forall\, n$ in (4) obeys the complex Gaussian distribution with the variance of σ_0^2. The prior distribution of each n-th target's angle is assumed to be the von Mises distribution with a mean of μ_k and a standard deviation of σ_{θ_k}, which is expressed as follows:

$$f(x|\mu,\kappa) = \frac{1}{2\pi I_0(\kappa)} \exp\{\kappa \cos(x-\mu)\}, \tag{25}$$

where x is the circular variable (e.g., angle), μ is the mean direction (a.k.a. the location parameter), and $\kappa = \frac{1}{\sigma_{\theta_n}^2}$ is the concentration parameter, which is analogous to the inverse of the variance in a normal distribution. $I_d(\kappa)$ is the modified Bessel function of order d. Note that the FIM for Gaussian distributions is the inverse of the covariance matrix when the variables are independent. Accordingly, we have the Bayesian *a priori* FIM as follows [22]

$$\mathbf{J}_P = \begin{bmatrix} \frac{1}{2\sigma_0^2} & 0 & 0 \\ 0 & \frac{1}{2\sigma_0^2} & 0 \\ 0 & 0 & \kappa \end{bmatrix}. \tag{26}$$

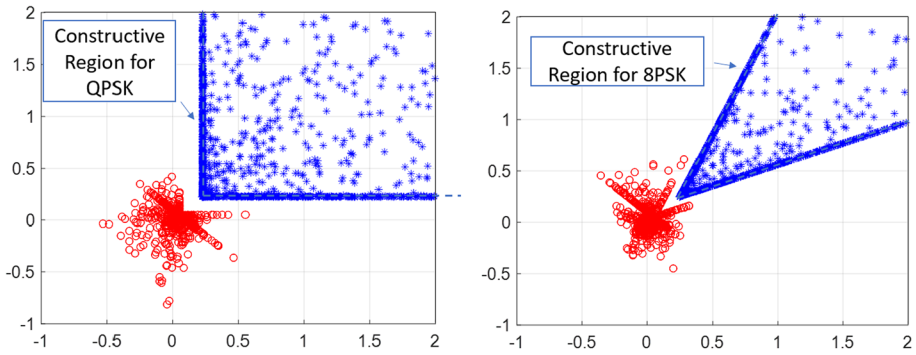

(a) QPSK (b) 8PSK

Fig. 2 The constellation of received signals at CUs, **a** QPSK, **b** 8PSK, $K_{cu} = 3, K_{tar} = 2, P_0 = 30$ dBm, $\Gamma_{\text{CU},k} = 15$ dB, $\forall\ k$, $\tau_{\text{E},n} = -5$ dB, and $\sigma_{\theta_n} = 5°, \forall\ n$

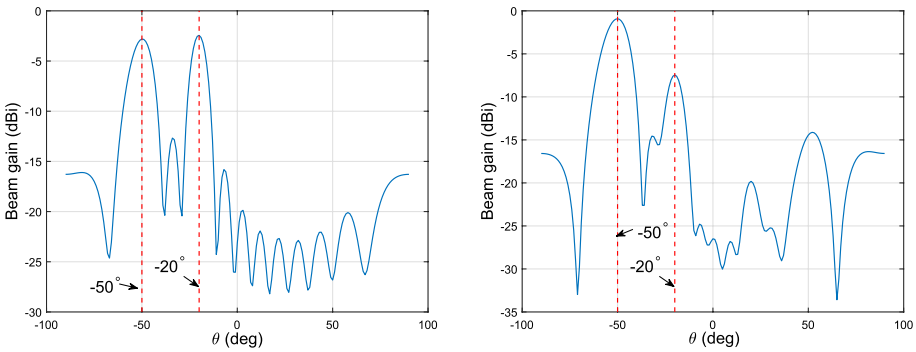

(a) $\sigma_{\theta_n} = 0.5°, \forall\ n$ (b) $\sigma_{\theta_n} = 5°, \forall\ n$

Fig. 3 The resultant beampatterns via the proposed secure ISAC signaling design with different *a priori* information of the angle, **a** standard deviation is 1°, **b** standard deviation is 5°, $K_{cu} = 3, K_{tar} = 2, P_0 = 30$ dBm, $\Gamma_{\text{CU},k} = 20$ dB$\forall\ k$

The spatial distribution of the received signals at CUs (denoted by blue dots) and at targets/Eves (denoted by red dots) is shown in Fig. 2, where QPSK and 8PSK modulated signals are taken as examples. The principal constellation points of the received signals for both CUs and targets/Eves on a 2D complex plane are illustrated. For CUs, the optimization process aligns symbols within the constructive interference region to maintain high decoding accuracy, ensuring reliable communications. In contrast, the received signals at the targets/Eves are forced into the destructive region, intentionally increasing the SER to enhance PLS by minimizing the probability of accurate decoding at their end.

In Fig. 3, we demonstrate the generated beampatterns with different standard deviations of the *a priori* information of the target angles. We assume that there exists in the field of interest $K_{tar} = 2$ targets located at $\theta_1 = -50°$ and $\theta_2 = -20°$, and the angle standard deviation is given as 1° and 5° in Fig. 3a and b, respectively. Figure 3 illustrates that the main lobes pointing to targets of interest get narrow and with higher beam gain when σ_{θ_n} gets smaller, which implies a higher accuracy of the target angle estimation.

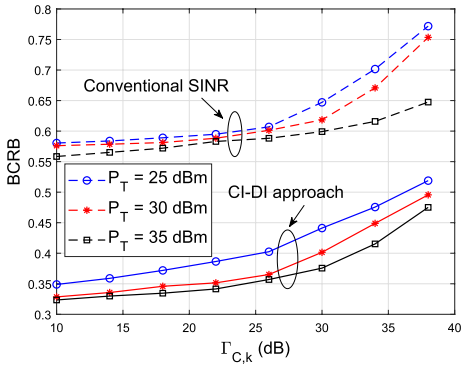

Fig. 4 Performance trade-off between the communication and sensing systems with different power budgets, for $K_{cu} = 3$ and $K_{tar} = 2$ and

Furthermore, Fig. 4 shows the trade-off between the communication and the sensing performances. It is obvious that with the improvement of the communication QoS, the CRB increases. In the block-level precoding, we leverage the conventional block-level SINR of the k-th CU as

$$\mathrm{SINR}_k = \frac{\left|\mathbf{h}_k^H \mathbf{w}_k\right|^2}{\sum_{i=1, i\neq k}^{K_{cu}} \left|\mathbf{h}_k^H \mathbf{w}_i\right|^2 + \sigma_{\mathrm{CU,k}}^2}, \tag{27}$$

where the signal matrix $\mathbf{X}$ in (3) can be written as $\mathbf{X} = \mathbf{WS}$, with $\mathbf{W}$ denoting the precoding matrix and $\mathbf{w}_k$ denoting the k-th entry of the precoding matrix $\mathbf{W}$ corresponding to the k-th CU, and the transmit signal vector $\mathbf{s}$ is a set to include QPSK-modulated symbols. The constraint $\mathrm{SINR}_k \geq \Gamma_k$ is equivalently rewritten as a convex second-order cone (SOC) constraints, which is given as $\sqrt{1+\Gamma_k}\,\mathbf{h}_k^H \mathbf{w}_k \geq \sqrt{\Gamma_k}\left\| \left[\mathbf{h}_k^H \mathbf{W}, \sigma_{\mathrm{CU,k}}\right] \right\|$ [23]. Afterward, by substituting (20c) and dropping (20d), the block-level precoding problem can be accordingly formulated as

$$\begin{aligned} &\min_{\mathbf{X}} \ \mathrm{tr}\left(\mathbf{J}^{-1}\right) \\ &\text{s.t.} \ \frac{1}{L}\|\mathbf{X}\|_F^2 \leq P_T, \\ &\sqrt{1+\Gamma_k}\,\mathbf{h}_k^H \mathbf{w}_k \geq \sqrt{\Gamma_k}\left\| \left[\mathbf{h}_k^H \mathbf{W}, \sigma_{\mathrm{CU,k}}\right] \right\|. \end{aligned} \tag{28}$$

The block-level precoding scheme in (27) is set as a benchmark in Fig. 4. It indicates that the proposed CI-DI-based design outperforms the block-level precoding technique, due to the reason that the block-level design consumes more power to reach the same SINR/SNR threshold, i.e., Γ_k.

Figure 5 depicts the average SER at CUs and targets/Eves versus the SNR threshold $\Gamma_{\mathrm{CU,k}}$. The proposed technique in [14] is set as a benchmark, which deploys the CI-DI algorithm while minimizing the reflected SINR. By imposing the DI constraints, we note that the SER at targets/Eves is close to one, which indicates that the communication data are effectively protected from being decoded by the targets/Eves. Besides, it also illustrated that the SER at CUs gets lower with an increasing power budget. Moreover, the BCRB optimization outperforms the benchmark technique, which reaches lower SER at the CUs.

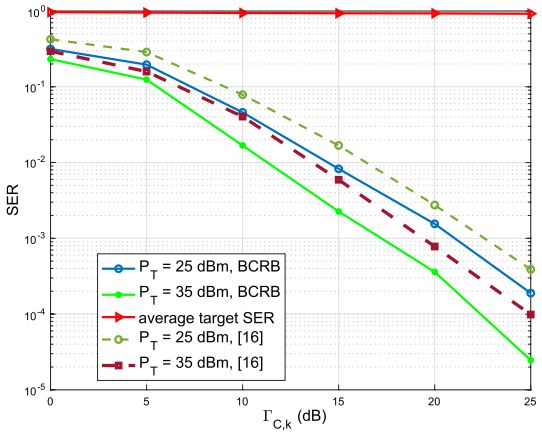

Fig. 5 SER of CUs and average SER of targets/Eves versus the SNR threshold $\Gamma_{CU,k}$ with different power budgets for $K_{cu} = 3$ and $K_{tar} = 2$

3 Conclusion

In this paper, we presented a novel symbol-level signaling design algorithm for ISAC systems aiming at ensuring communication data security. The proposed design exploits the CI-DI technique, while sensing performance was measured by the BCRB and its PLS capability was quantified by the SER. Our optimization problem formulation deals with the BCRB minimization, while conveying the received signals at CUs into the constructive region and making sure the received signals at targets/Eves fall into the destructive region. The presented numerical results verified that the CI-DI technique effectively protects communication data security. It was also showcased that the proposed symbol-level precoding technique outperforms the block-level precoding design. It was also demonstrated that the resultant beampattern with the proposed design yields improved sensing performance (i.e., narrower main beam with higher beam gain) when a priori statistical information of the unknown targets' parameters is known accurately.

Abbreviations

AN	Artificial noise
AWGN	Additive white Gaussian noise
BCRB	Bayesian Cramér–Rao bound
BFIM	Bayesian Fisher Information Matrix
BS	Base station
CI	Constructive interference
CU	Communication user
DM	Directional modulation
ISAC	Integrated sensing and communication
MIMO	Multi-input multi-output
MSE	Mean-squared error
NLS	Network layer security
PLS	Physical layer security
PSK	Phase-shift keying
QoS	Quality of service
R &C	Radar and communication
RCS	Radar cross section
RIS	Reconfigurable intelligent surfaces
S &C	Sensing and communication

Author contributions

All authors made contributions to the discussions, analysis, and implementation of the proposed solution. All authors read and approved the final manuscript.

Funding
This work was supported in part by the Engineering and Physical Sciences Research Council (EPSRC) under Grant EP/S028455/1, in part by the National Natural Science Foundation of China under Grant 62101234, Grant 62401181, Grant U20B2039, Grant 61831008 and Grant 62027802, in part by the Young Elite Scientist Sponsorship Program by CAST under Grant No. YESS20210055, and in part by Smart Networks and Services Joint Undertaking (SNS JU) project 6 G-DISAC under the European Union's Horizon Europe research and innovation program under Grant Agreement no. 101139130.

Data availability
Not applicable.

Declarations

Competing interests
Christos Masouros, George C. Alexandropoulos, and Fan Liu are Guest Editors for EURASIP Journal on Wireless Communications and Networking and were not involved in the editorial review or the decision to publish this article. The authors declare no other conflict of interest.

Received: 11 July 2024 Accepted: 16 January 2025
Published online: 27 February 2025

References

1. F. Liu, L. Zheng, Y. Cui, C. Masouros, A.P. Petropulu, H. Griffiths, Y.C. Eldar, Seventy years of radar and communications: the road from separation to integration. IEEE Signal Process. Mag. **40**(5), 106–121 (2023)
2. S.P. Chepuri, N. Shlezinger, F. Liu, G.C. Alexandropoulos, S. Buzzi, Y.C. Eldar, Integrated sensing and communications with reconfigurable intelligent surfaces: from signal modeling to processing. IEEE Signal Process. Mag. **40**(6), 41–62 (2023)
3. A. Liu, Z. Huang, M. Li, Y. Wan, W. Li, T.X. Han, C. Liu, R. Du, D.K.P. Tan, J. Lu et al., A survey on fundamental limits of integrated sensing and communication. IEEE Commun. Surv. Tutorials **24**(2), 994–1034 (2022)
4. N. Su, F. Liu, C. Masouros, Sensing-assisted eavesdropper estimation: An ISAC breakthrough in physical layer security. IEEE Transactions on Wireless Communications (2023)
5. N. Su, F. Liu, C. Masouros, Secure radar-communication systems with malicious targets: Integrating radar, communications and jamming functionalities. IEEE Trans. Wireless Commun. **20**(1), 83–95 (2020)
6. G.C. Alexandropoulos, K.D. Katsanos, M. Wen, D.B. Da Costa, Counteracting eavesdropper attacks through reconfigurable intelligent surfaces: A new threat model and secrecy rate optimization. IEEE Open Journal of the Communications Society (2023)
7. X. Zhu, J. Liu, L. Lu, T. Zhang, T. Qiu, C. Wang, Y.Liu, Enabling intelligent connectivity: A survey of secure ISAC in 6G networks. IEEE Communications Surveys & Tutorials (2024)
8. Z. Ren, L. Qiu, J. Xu, Optimal transmit beamforming for secrecy integrated sensing and communication. In: ICC 2022-IEEE International Conference on Communications, pp. 5555–5560 (2022). IEEE
9. Y. Liu, L. Li, G.C. Alexandropoulos, M. Pesavento, Securing relay networks with artificial noise: an error performance-based approach. Entropy **19**(8), 384 (2017)
10. A. Bazzi, M. Chafii, Secure full duplex integrated sensing and communications. IEEE Transactions on Information Forensics and Security (2023)
11. R. Liu, M. Li, Q. Liu, A.L. Swindlehurst, Secure symbol-level precoding in MU-MISO wiretap systems. IEEE Trans. Inf. Forensics Secur. **15**, 3359–3373 (2020)
12. Z. Wei, C. Masouros, F. Liu, S. Chatzinotas, B. Ottersten, Energy-and cost-efficient physical layer security in the era of IoT: the role of interference. IEEE Commun. Mag. **58**(4), 81–87 (2020)
13. M. Alodeh, S. Chatzinotas, B. Ottersten, Constructive multiuser interference in symbol level precoding for the MISO downlink channel. IEEE Trans. Signal Process. **63**(9), 2239–2252 (2015)
14. N. Su, F. Liu, Z. Wei, Y.-F. Liu, C. Masouros, Secure dual-functional radar-communication transmission: Exploiting interference for resilience against target eavesdropping. IEEE Transactions on Wireless Communications (2022)
15. B. Smida, A. Sabharwal, G. Fodor, G.C. Alexandropoulos, H.A. Suraweera, C.-B. Chae, Full-duplex wireless for 6G: Progress brings new opportunities and challenges. IEEE Journal on Selected Areas in Communications (2023)
16. G.C. Alexandropoulos, M.A. Islam, B. Smida, Full-duplex massive multiple-input, multiple-output architectures: Recent advances, applications, and future directions. IEEE Vehicular Technology Magazine (2022)
17. C. Masouros, G. Zheng, Exploiting known interference as green signal power for downlink beamforming optimization. IEEE Trans. Signal Process. **63**(14), 3628–3640 (2015)
18. Y. Xiong, F. Liu, Y. Cui, W. Yuan, T.X. Han, G. Caire, On the fundamental tradeoff of integrated sensing and communications under Gaussian channels. IEEE Transactions on Information Theory (2023)
19. Q. Xu, P. Ren, A.L. Swindlehurst, Rethinking secure precoding via interference exploitation: a smart eavesdropper perspective. IEEE Trans. Inf. Forensics Secur. **16**, 585–600 (2020)
20. M.R. Khandaker, C. Masouros, K.-K. Wong, S. Timotheou, Secure SWIPT by exploiting constructive interference and artificial noise. IEEE Trans. Commun. **67**(2), 1326–1340 (2018)
21. S.P. Boyd, L. Vandenberghe, Convex optimization (2004)
22. A. Vempaty, H. He, B. Chen, P.K. Varshney, On quantizer design for distributed Bayesian estimation in sensor networks. IEEE Trans. Signal Process. **62**(20), 5359–5369 (2014)
23. F. Liu, Y.-F. Liu, C. Masouros, A. Li, Y.C. Eldar, A joint radar-communication precoding design based on Cramér-Rao bound optimization. In: 2022 IEEE Radar Conference (RadarConf22), pp. 1–6 (2022). IEEE

Publisher's Note
Springer Nature remains neutral with regard to jurisdictional claims in published maps and institutional affiliations.